

**Stem Cell Reports, Volume 2**

**Supplemental Information**

**Exosomes as Critical Agents of Cardiac**

**Regeneration Triggered by Cell Therapy**

**Ahmed Gamal-Eldin Ibrahim, Ke Cheng, and Eduardo Marbán**

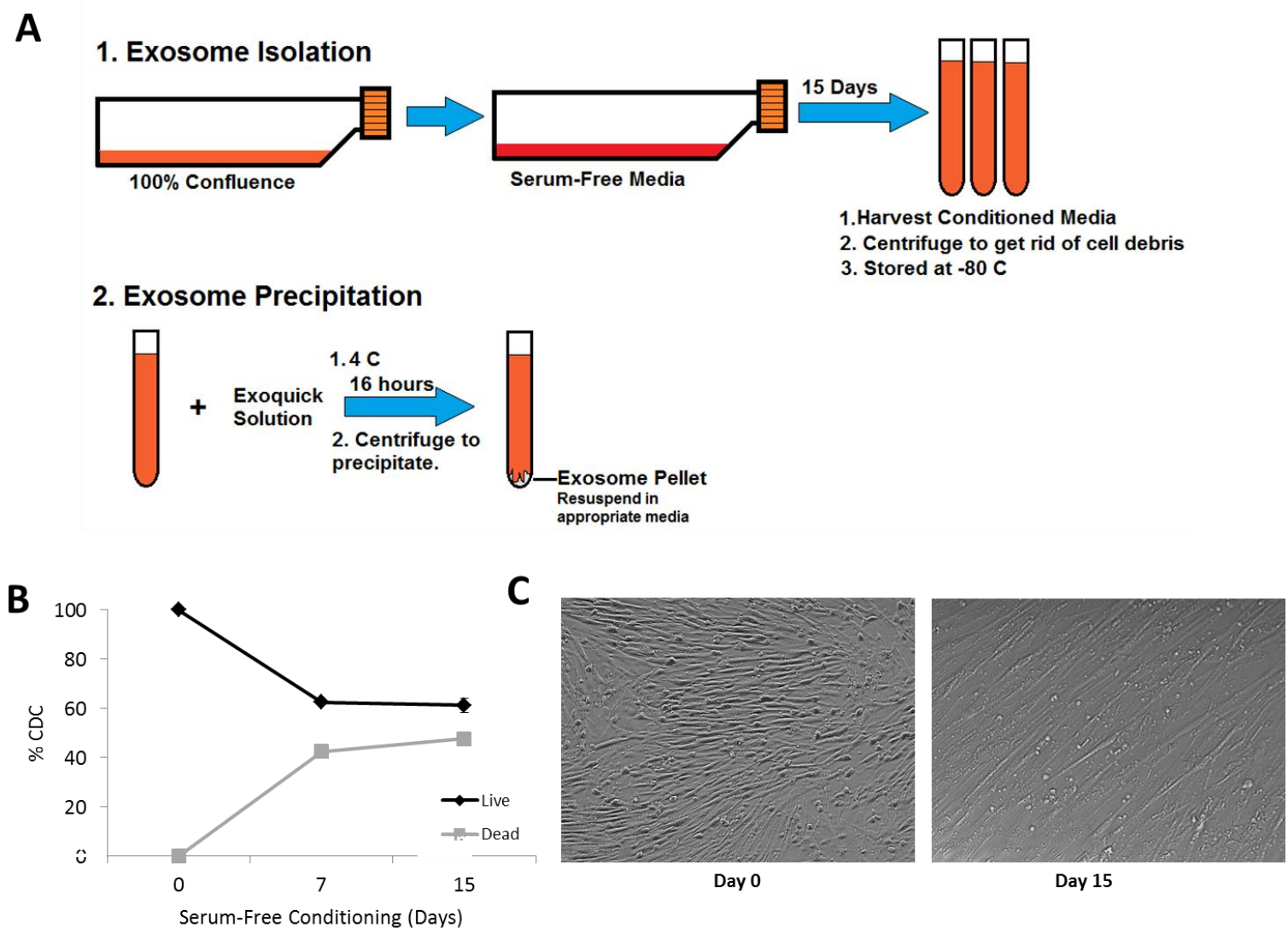
## **Supplemental Discussion**

### **Differences in baseline ejection fraction between different mouse strains**

We noted a noticeably high baseline ejection fraction for these animals. We surmise that this difference is due to the different background strain of mice used in the knockouts (C57BL6). In all other experiments in the manuscript, the strain of mice used is SCID-Beige. SCID-Beige mice lack mature B and T cells as well as Natural Killer (NK) cells. This fundamental difference in immune competence likely accounts for the contrast in the baseline measurement as they respond to injury differently. In most of the experiments in this manuscript we chose the SCID-Beige mouse since they are permissive to human cells (which are the source of the CDC and the exosomes). However an appropriate control for the 146a KO mouse was a wild type from the same background strain which the BL6 background. This has been previously documented. Strain has previously been shown to be a significant determinant of wound healing after myocardial infarction (van den Borne et al., 2009).

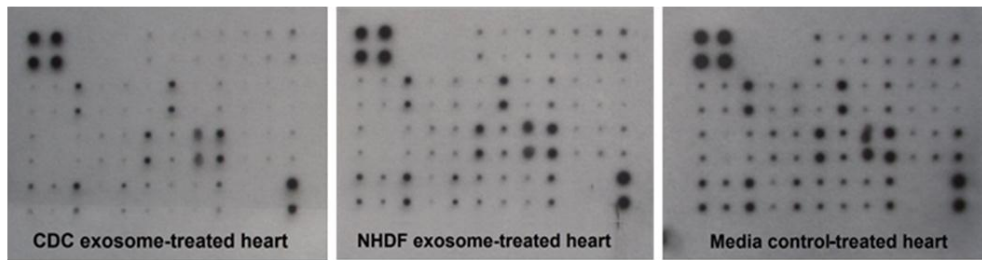
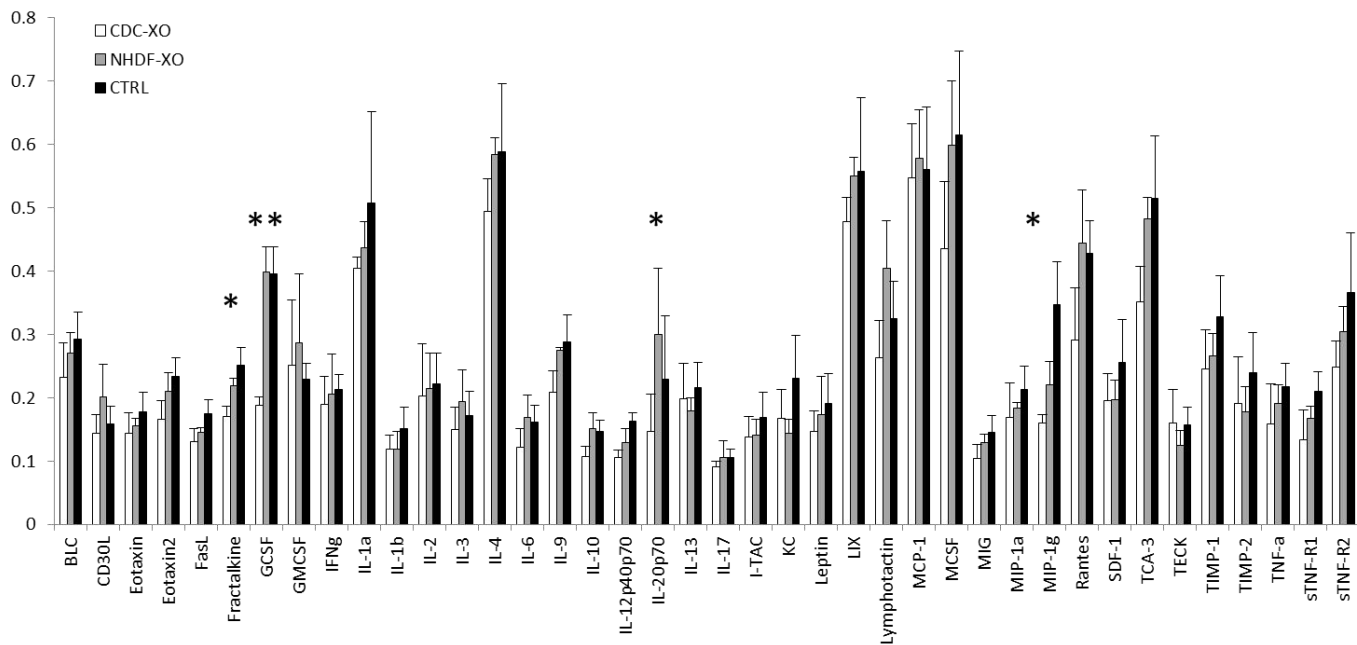
### **MiR-146a effect on immune infiltration**

Attenuating the inflammatory immune response is not necessarily abrogating it altogether. Innate immune cells including macrophages have been shown to play pro regenerative roles. Furthermore unpublished data from our lab show that macrophage trafficking is not affected by CDC treatment, but macrophages treated with CDCs do switch from an M1 (proinflammatory) to an anti-inflammatory and pro-healing phenotype M2.



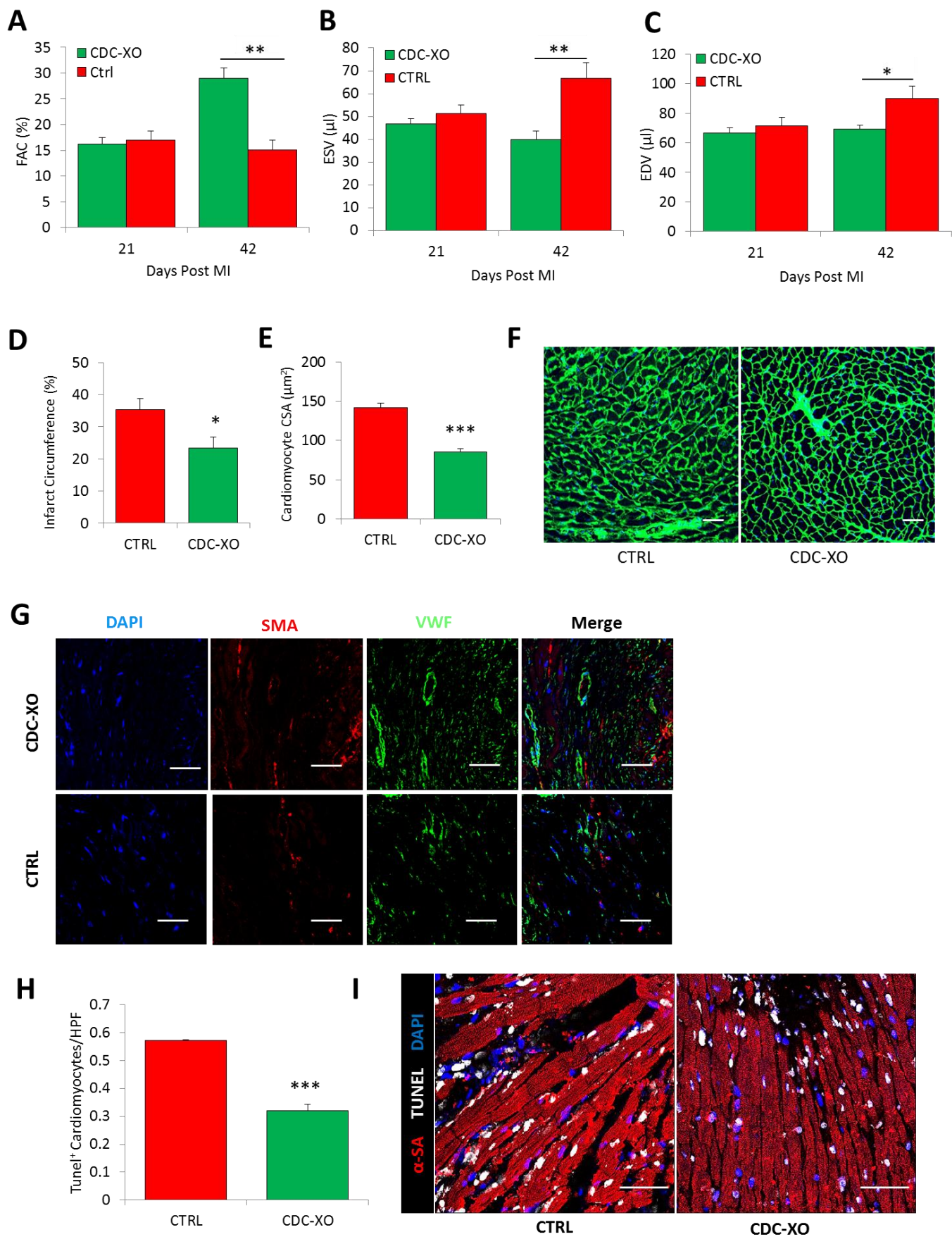
**Figure S1. Isolation of exosomes from Cardiosphere-derived cells, Related to Figure 1**

(A) Graphical representation of exosome isolation and purification for exosomes. (B) Cell viability (calcein) and cell death (Ethidium homodimer-1) assay performed on CDCs over the 15 day serum-free conditioning period. (C) Representative images of CDCs before and after serum-free conditioning.

**A****B**

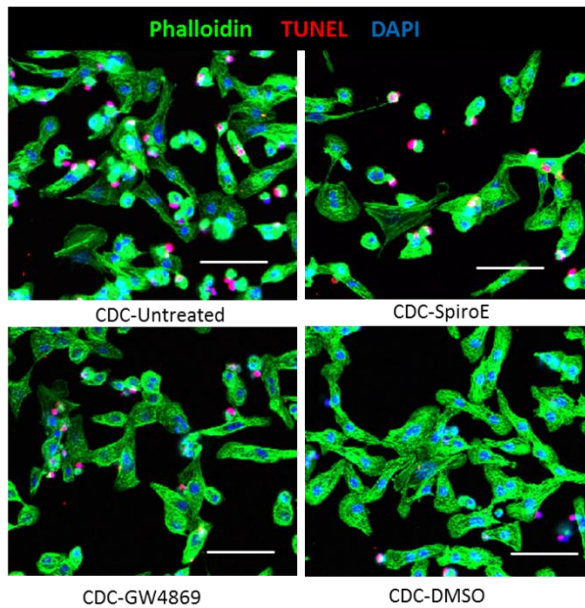
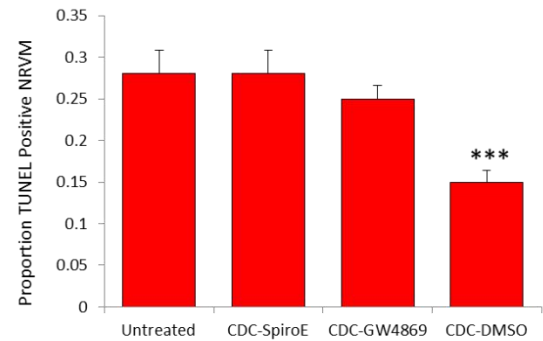
**Figure S2. CDC exosomes reduce inflammation in a mouse model of acute MI, Related to Figure 2**

(A) Representative protein arrays for 40 pro-inflammatory markers. (B) Quantification of inflammatory proteins in mouse hearts treated with CDC-exosomes, NHDF-exosomes, or control. Data comes from three mouse hearts per group. Analysis was done using one-way ANOVA (95% CI) (n=3 hearts per group). Data represented as mean and standard error of the mean.



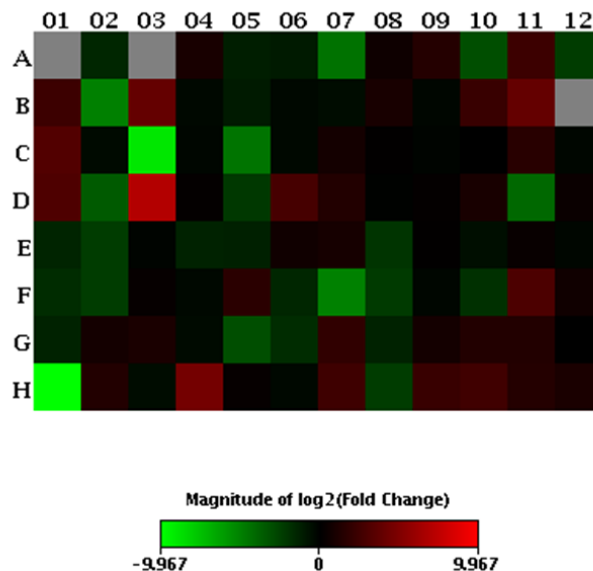
**Figure S3. CDC-exosomes produce structural and functional benefits in mouse hearts after MI,  
Related to Figure 2**

CDC-exosomes stimulate functional improvement and attenuate adverse remodeling and cardiac hypertrophy in a mouse model of chronic MI (a) Animals treated with CDC-exosomes showed significant functional improvement compared to control as shown by fractional area change (A) , end systolic volume (B) and end diastolic volume (C) (A-C, n=6 animals per group). Animals treated with CDC-exosomes also showed structural improvements as noted as seen in percent of the circumference of tissue sections that are scar (D), decreased cardiomyocyte hypertrophy (E) as measured by staining with wheat germ agglutinin and DAPI (F) and increased angiogenesis in the infarct zone (G). Less cardiomyocyte death was observed in the border zone of CDC-exosome-treated animals compared to control. (H, I) (D-I n=4 hearts per group) \*P<0.05, \*\*P<0.01, \*\*\*P<0.001. using Student's t test, all scale bars represent 50  $\mu$ m. Data represented as mean and standard error of the mean.

**A****B**

**Figure S4. Inhibition of exosome secretion in CDCs diminishes the protective effects of CDCs in vitro, Related to Figure 3**

Neonatal rat ventricular myocytes were stressed with 50  $\mu\text{M}$   $\text{H}_2\text{O}_2$  for 15 minutes followed by trans-well treatment with CDCs pre-treated with 5  $\mu\text{M}$  of Spiroepoxide, 20  $\mu\text{M}$  of GW4869, or vehicle (DMSO). (A) Cell death was measured using TUNEL staining (red), Phalloidin (green), and DAPI (blue). (B) Pooled data of the four groups represented as proportion of TUNEL positive cardiomyocyte nuclei of total cells counted ( $n=3$  technical replicates from neonatal rat cardiomyocytes derived from 20-30 rat pups from 3 different mothers) (B). \* $P<0.05$ , \*\* $P<0.01$ , \*\*\* $P<0.001$  using Student's  $t$  test, all scale bars represent 50  $\mu\text{m}$ . Data represented as mean and standard error of the mean.



A01 hsa-miR-142-5p	A02 hsa-miR-16	A03 hsa-miR-142-3p	A04 hsa-miR-21	A05 hsa-miR-15a	A06 hsa-miR-29b	A07 hsa-let-7a	A08 hsa-miR-126	A09 hsa-miR-143	A10 hsa-let-7b	A11 hsa-miR-27a	A12 hsa-let-7f
B01 hsa-miR-9	B02 hsa-miR-26a	B03 hsa-miR-24	B04 hsa-miR-30e	B05 hsa-miR-181a	B06 hsa-miR-29a	B07 hsa-miR-124	B08 hsa-miR-144	B09 hsa-miR-30d	B10 hsa-miR-19b	B11 hsa-miR-22	B12 hsa-miR-122
C01 hsa-miR-150	C02 hsa-miR-32	C03 hsa-miR-155	C04 hsa-miR-140-5p	C05 hsa-miR-125b	C06 hsa-miR-141	C07 hsa-miR-92a	C08 hsa-miR-424	C09 hsa-miR-191	C10 hsa-miR-17	C11 hsa-miR-130a	C12 hsa-miR-20a
D01 hsa-miR-27b	D02 hsa-miR-26b	D03 hsa-miR-146a	D04 hsa-miR-200c	D05 hsa-miR-99a	D06 hsa-miR-19a	D07 hsa-miR-23a	D08 hsa-miR-30a	D09 hsa-let-7i	D10 hsa-miR-93	D11 hsa-let-7c	D12 hsa-miR-106b
E01 hsa-miR-101	E02 hsa-let-7g	E03 hsa-miR-425	E04 hsa-miR-15b	E05 hsa-miR-28-5p	E06 hsa-miR-18a	E07 hsa-miR-25	E08 hsa-miR-23b	E09 hsa-miR-302a	E10 hsa-miR-186	E11 hsa-miR-29c	E12 hsa-miR-7
F01 hsa-let-7d	F02 hsa-miR-30c	F03 hsa-miR-181b	F04 hsa-miR-223	F05 hsa-miR-320a	F06 hsa-miR-374a	F07 hsa-let-7e	F08 hsa-miR-151-5p	F09 hsa-miR-374b	F10 hsa-miR-196b	F11 hsa-miR-140-3p	F12 hsa-miR-100
G01 hsa-miR-103	G02 hsa-miR-96	G03 hsa-miR-302b	G04 hsa-miR-194	G05 hsa-miR-125a-5p	G06 hsa-miR-423-5p	G07 hsa-miR-376c	G08 hsa-miR-195	G09 hsa-miR-222	G10 hsa-miR-28-3p	G11 hsa-miR-128	G12 hsa-miR-302c
H01 hsa-miR-423-3p	H02 hsa-miR-185	H03 hsa-miR-30b	H04 hsa-miR-210	H05 SNORD48							

**Figure S5. Heat map of MiR PCR array identifies miR-146a as the most differentially expressed miR, Related to Figure 4**

Heat map showing fold regulation differential abundance data for transcripts between CDC exosomes and NHDF exosomes overlaid onto the PCR Array plate layout.



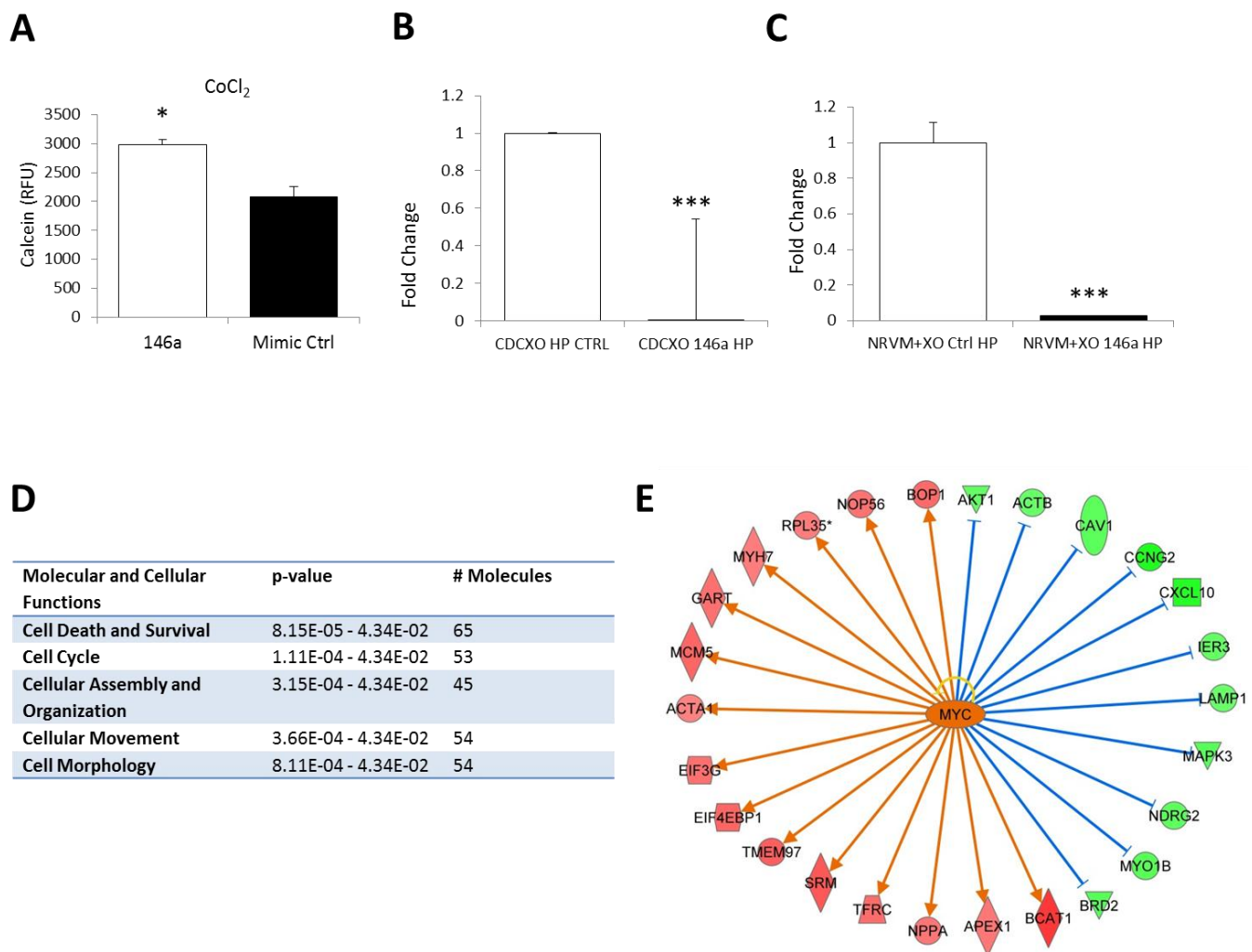


**Figure S6. miR-146a protects stressed neonatal rat cardiomyocytes, Related to Figures 4 and 5**

(A) Cardiomyocytes were pre-treated with 80 nM miR-146a mimic or mimic-control then exposed to 5 mM cobalt chloride for 2 hours (n=4 technical replicates per group of neonatal rat cardiomyocytes derived from 20-30 rat pups from 3 different mothers) (B, C) CDC exosomes derived from CDCs transfected with mir-146a hairpin inhibitor. Exosomes were derived from conditioned media and mir-146a knockdown confirmed by qPCR in exosomes. (C) Decreased levels of mir-146a in NRVMs treated with 146a-free exosomes compared to control (n=3 technical replicates per group of neonatal rat cardiomyocytes derived from 20-30 rat pups from 3 different mothers). Pathway analysis derived from transcriptome data showing affected pathways and (B) Pathway depiction showing MYC activation as a putative hub, based on microarray data analysis.

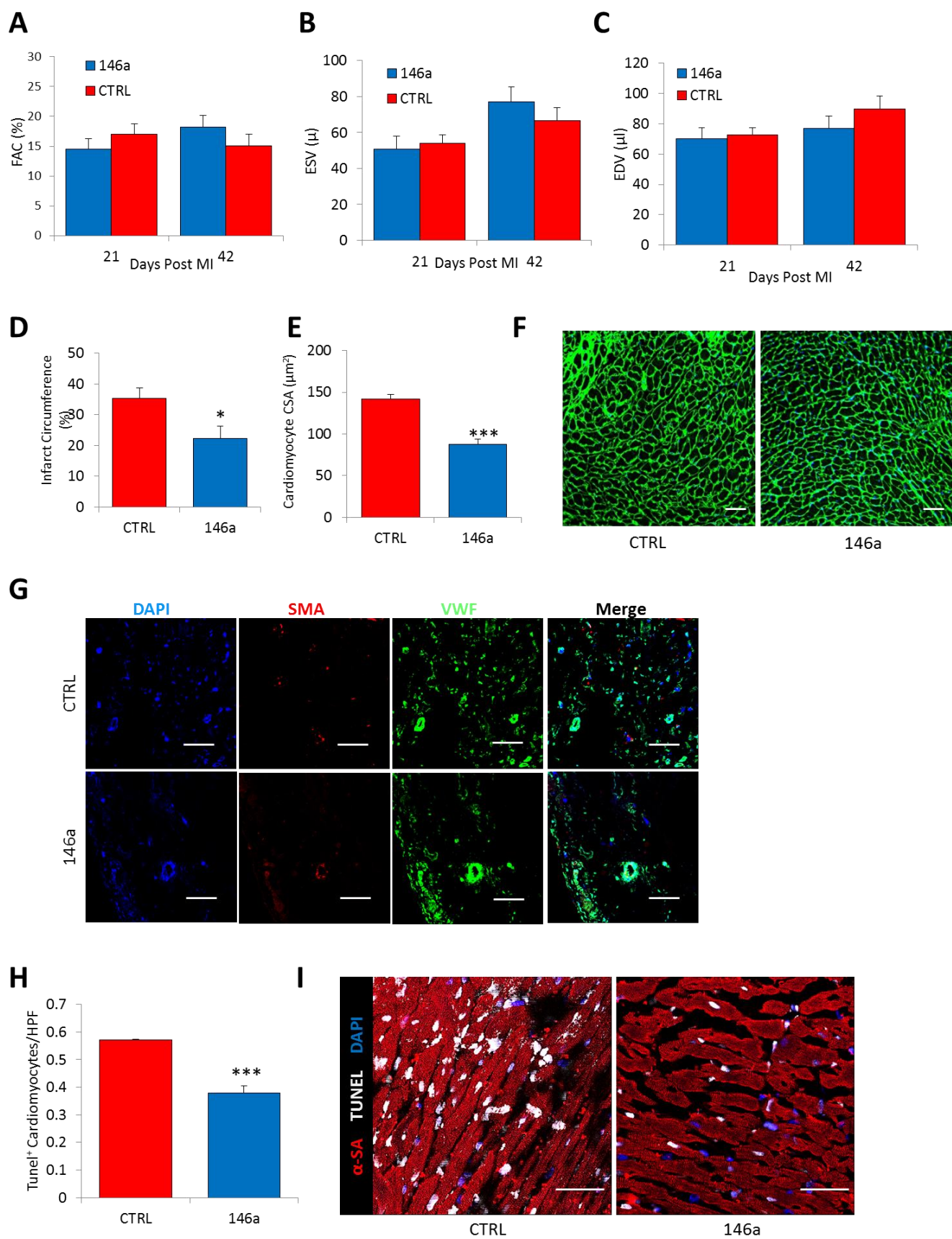


**Figure S7. MiR-146a reproduces some but not all the effects of CDC-exosomes, Related to Figure 5**

MiR-146a attenuates adverse remodeling and cardiac hypertrophy in a mouse model of chronic MI. (A-C) Animals treated with CDC-exosomes showed no significant functional improvement compared to control as shown by fractional area change (A), end systolic volume (B) and end diastolic volume (C) (A-C, n= 6 animals per group). Structural improvements however were noted as seen in percent of the circumference of tissue sections that are scar (D), and decreased cardiomyocyte hypertrophy (E) as measured by staining with wheat germ agglutinin and DAPI. No differences in angiogenesis were observed between the two groups (G). Less cardiomyocyte death was observed in the border zone of mir 146a-treated animals compared to control. (H, I) (D-I, n=4 hearts per group) \*P<0.05, \*\*P<0.01, \*\*\*P<0.001 using Student's t test, all scale bars represent 50  $\mu$ m. Data represented as mean and standard error of the mean.